applied sciences

MDPI

Article

Packed Bed Photoreactor for the Removal of Water Pollutants Using Visible Light Emitting Diodes

Olga Sacco, Diana Sannino and Vincenzo Vaiano *

Department of Industrial Engineering, University of Salerno, Via Giovanni Paolo II 132, 84084 Fisciano, Italy; osacco@unisa.it (O.S.); dsannino@unisa.it (D.S.)

* Correspondence: vvaiano@unisa.it; Tel.: + 39-089-964006

Received: 3 January 2019; Accepted: 25 January 2019; Published: 30 January 2019

Abstract: A packed bed photoreactor was developed using a structured photocatalyst active under visible light. The packed bed reactor was irradiated by visible light-emitting diodes (LEDs) for the evaluation of photocatalytic activity in the removal of different types of water pollutants. By using a flexible LEDs strip as the external light source, it was possible to use a simple cylindrical geometry for the photoreactor, thereby enhancing the contact between the photocatalyst and the water to be treated. The visible light active structured photocatalyst was composed by N-doped TiO_2 particles supported on polystyrene spheres. Photocatalytic results showed that the almost total methylene blue decolorization was achieved after 120 min of irradiation. Moreover, the developed packed bed photoreactor was effective in the removal of ceftriaxone, paracetamol, and caffeine, allowing it to reach the almost total degradation of the pollutants and a total organic carbon removal above 80% after 180 min of visible light irradiation.

Keywords: packed bed photoreactor; visible LEDs; visible light active structured photocatalyst; water and wastewater treatment

1. Introduction

The main causes of water contamination are industrial discharges, excess use of pesticides and fertilizers, the presence of pharmaceutical residues, and landfilling of domestic wastes [1]. Traditional water treatment processes are mainly based on mechanical (sedimentation and filtration), biological, and physical–chemical processes (flocculation, sterilization, or chemical oxidation) [2,3]. Advanced treatment technologies are based on the pollutants oxidation by potassium permanganate, ozone, hydrogen peroxide, high-energy ultraviolet light, photo-Fenton, electro-Fenton, and photo-electro-Fenton processes [4–8]. Typically, these technologies are not cost-effective [9]. On the other hand, the conventional wastewater treatments have different disadvantages, such as use of chemicals and production of sludge, as well as low efficiency in removal of bio-recalcitrant compounds [10]. Heterogeneous photocatalysis is one of the advanced oxidation processes that couples low-energy light with semiconductors acting as photocatalysts and, therefore, it could be considered as sustainable process for the treatment and purification of water and wastewater [11,12]. Although in recent years, a large number of publications have shown the potential of photocatalytic treatment for the removal of different categories of toxic compounds in water [13–15] using also innovative photoreactors configurations [16–18], the research is still limited to the development of photocatalytic laboratory reactors or to photoreactors very difficult to scale up. It must be considered that the design of a photocatalytic reactor is not an easy step; in particular, the development of a photocatalytic reactor is complicated because it is necessary to have an adequate irradiation of the overall reaction volume for the activation of the entire mass of photocatalyst and to favor an easy catalyst separation after treatment [19]. Typically, these reactors are designed to study the photocatalytic degradation

of pollutants through the application of conventional lamps as light sources [20]. However, since conventional lamps are expensive in terms of manufacturing, as well as electricity consumption, many studies have been devoted to photocatalytic reactors that exploit the solar spectrum [21].

But it is necessary to take into account the many limitations related to solar photoreactors. For example, in a solar compound parabolic collector (CPC), despite the fact that the reactor is formed by small tubes, the area equipped by the parabolic collector for light harvesting is huge. So, the installation of these systems also requires a large area [22] to avoid that the single modules projecting shadows upon each other [23]. Another limitation this kind of system is connected to the use of only direct sunlight [24,25]. Thus, the solar photoreactors do not work efficiently during cloudy days and night time. The recent rapid advances in light-emitting diodes (LEDs) technology have made possible a new frontier for a wide range of lighting applications, including photocatalysis and, consequently, photoreactor design [26,27]. In fact, the energy conversion efficiency of LEDs has increased exponentially in recent years, making them a suitable light source for the design of compact photocatalytic reactors for water and wastewater treatment [28,29], as well as for the removal of hazardous compounds from gaseous streams [30], overcoming the limitations related to the developing of photocatalytic reactors into pilot scale level. With the use of LEDs, the design of photoreactors could be significantly facilitated and, by using a flexible LEDs strip as the external light source, it is possible to use simple cylindrical geometry for photoreactor, thereby enhancing the contact between the photocatalyst and the water to be treated.

Moreover, cylindrical geometry for photocatalytic reactors is the most used in solar through collectors [31], and it is the simplest configuration, allowing a possible scale-up of photocatalytic systems for water and wastewater treatment.

Considering all the aspects describe above, the aim of this paper is to develop a cylindrical packed bed photoreactor at semi-pilot scale irradiated by visible LEDs and using a visible light active structured photocatalyst. The visible light active structured photocatalyst is composed by N-doped TiO_2 supported on polystyrene (PS) spheres [32,33] in order to avoid a post-separation step necessary for the separation of the photocatalyst from the treated water. The photocatalytic system has been tested in the removal of different types of water pollutants (methylene blue (MB), caffeine (CAF), paracetamol (PC), and ceftriaxone (CFX)).

2. Results and Discussion

2.1. Discoloration and Mineralization of Methylene Blue with the Packed Bed Photoreactor Operating in Batch Mode

Preliminary experiments were carried out while operating in batch mode (Figure 1) in order to verify that methylene blue (MB) was degraded by the heterogeneous photocatalytic process.

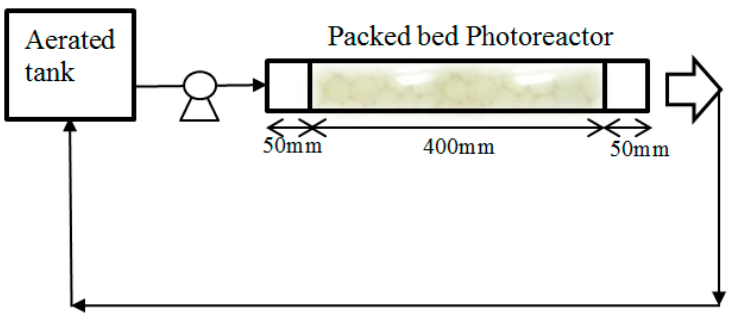

Figure 1. Schematic picture of the packed bed photoreactor working in batch mode.

The obtained results are reported in Figure 2. In the absence of a structured catalyst, no significant decrease in MB concentration was observed during the overall irradiation time, evidencing that the visible light was not able to degrade the MB molecule. A completely different behaviour was observed

when N-TiO_2/PS structured photocatalyst was placed into the photoreactor. In fact, the MB relative concentration gradually decreased in the run time and almost complete decolorization was achieved after 120 min of visible light irradiation. Several published papers have reported the removal of MB with fixed bed photoreactors irradiated by artificial light sources, as well as with solar photocatalytic reactors using structured photocatalysts (Table 1) [34–38]. For example, almost total MB decolorization was achieved after 48 h in the solar photoreactor proposed by Sutisna et al. [34], in which TiO_2 nanoparticles were placed as coating on transparent granules and used in the prototype of a flat-panel photoreactor. El-Mekkawi et al. [35] observed the complete decolorization after 5 h under the sunlight irradiation using a solar concentrator photoreactor prototype with TiO_2 deposited on polyethylene terephthalate (PET) textile substrate sheets. In some cases, it was reported that MB degraded more than 96% in up to 90 min of reaction using TiO_2 immobilized on glass spheres [36]. However, the same authors used a lab scale compound parabolic collector reactor irradiated by lamp at high electrical power (300 W) simulating the solar spectrum.

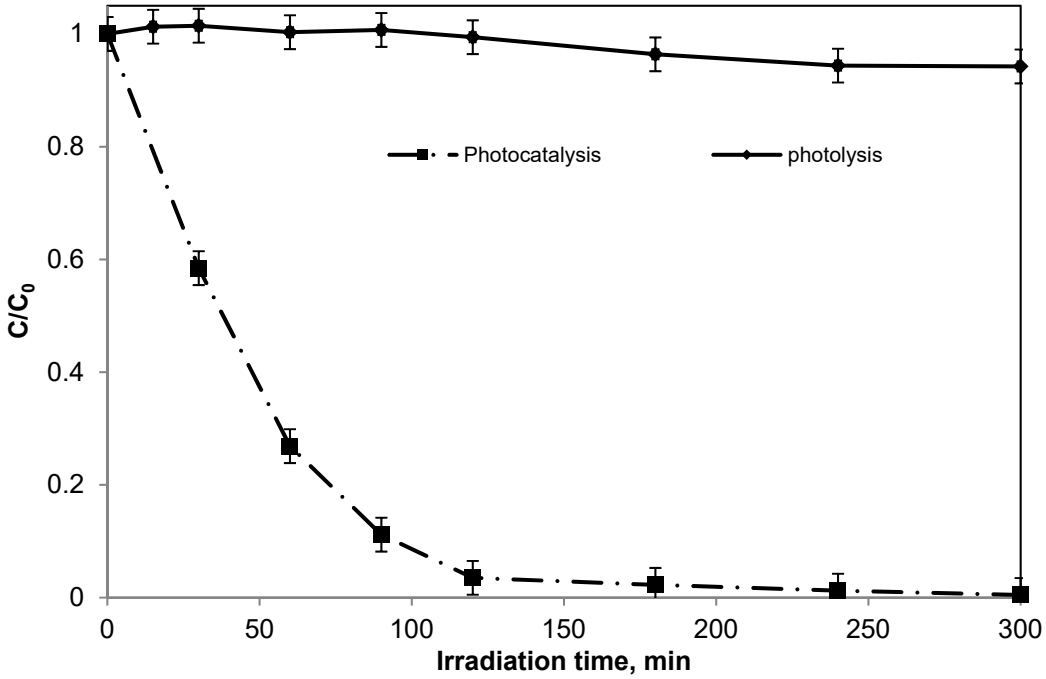

Figure 2. Behavior of methylene blue (MB) relative concentration as function of irradiation time for N-TiO2/polystyrene (PS) and photolysis test. Light sources: visible light-emitting diodes (LEDs); light intensity: 78 mW/cm_2; initial MB concentration: 7 mg/L; liquid flow rate: 50 mL/min; photoreactor configuration: batch mode.

As observed in our previous work [33], the performances of the photocatalytic system were not influenced by mass transfer limitation phenomena of MB dye from the aqueous phase to the photoactive surface, evidencing that the MB photocatalytic degradation rate is controlled by kinetics. In addition, after 300 min of visible light irradiation, the system allowed to achieve a total organic carbon (TOC) removal of 85±2% for all the liquid flow rates (Figure 3). Similar behaviours were observed for other photocatalytic systems in which the photoactive phases were immobilized on macroscopic supports [38,39]. In order to verify the stability of the structured photocatalyst, the photocatalytic degradation of MB was replicated up to four cycles. Before each reuse cycle, any cleaning or regenerating step of the structured photocatalyst was performed.

Table 1. Comparison with studies reported in the literature dealing with a different fixed bed photoreactor for methylene blue removal irradiated by artificial light sources, as well as with solar photocatalytic reactors using structured photocatalysts; PET (Polyethylene Terephthalate).

Catalyst	Catalyst Size	Initial MB Concentration (mg/L)	Light Source	Treatment Time *	Reusability	References
TiO_2/plastic granules	3.5 mm	25	Solar light	>48 h	Not reported	[34]
TiO_2/PET	2 × 7 cm	5	Solar light	5 h	Not reported	[35]
TiO_2/glass spheres	5 mm	10	Solar simulator	>1.5 h	Decrease of activity	[36]
TiO_2/polypropylene	3.5 mm	25	Solar light	6 h	Not reported	[37]
N-TiO_2/glass spheres	1 cm	10	Visible light lamps	>6.5 h	Not reported	[38]

* Time to reach a total MB decolorization.

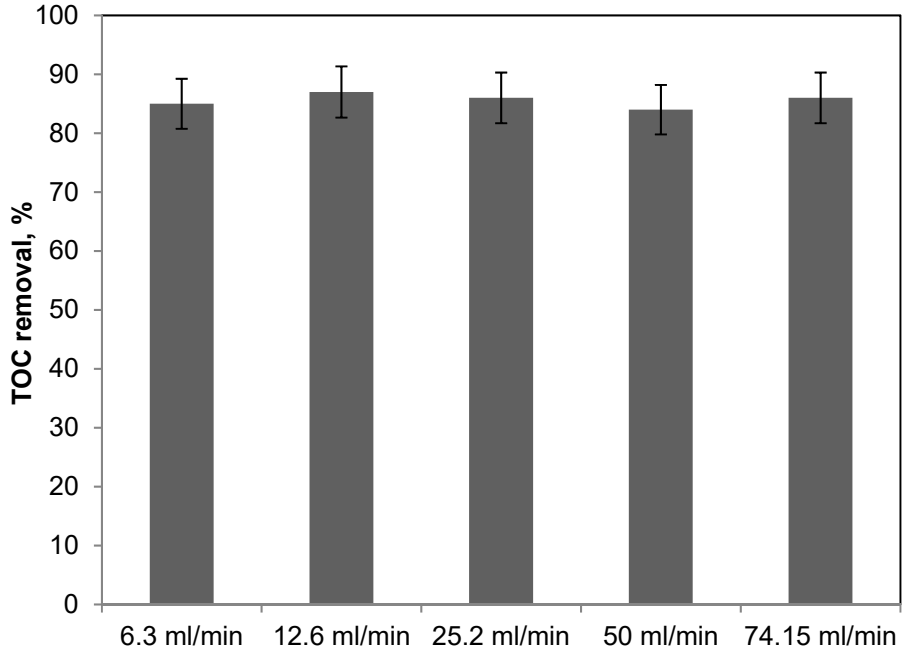

Figure 3. Behavior of MB relative concentration as function of irradiation time at different liquid flow rate. Light sources: visible LEDs; light intensity: 78 mW/cm^2; initial MB concentration: 7 mg/L; photoreactor configuration: batch mode; and total organic carbon (TOC).

The treated solution was removed from the photoreactor, and a fresh solution with the same initial MB concentration was fed for a new test. The MB decolorization and total organic carbon (TOC) removal was analyzed after 300 min visible light irradiation and the obtained results are shown in Figure 4.

From the comparison between the first cycle (when N-TiO_2/PS was fresh) and the fourth cycle, it was possible to observe that the photocatalytic activity was similar. This result indicated that N-TiO_2/PS did not deactivate after its reuse and no loss of photocatalyst particles from the polymer surface occurred, in agreement with previous results observed on structured photocatalysts prepared through solvent-casting method [32,33,40].

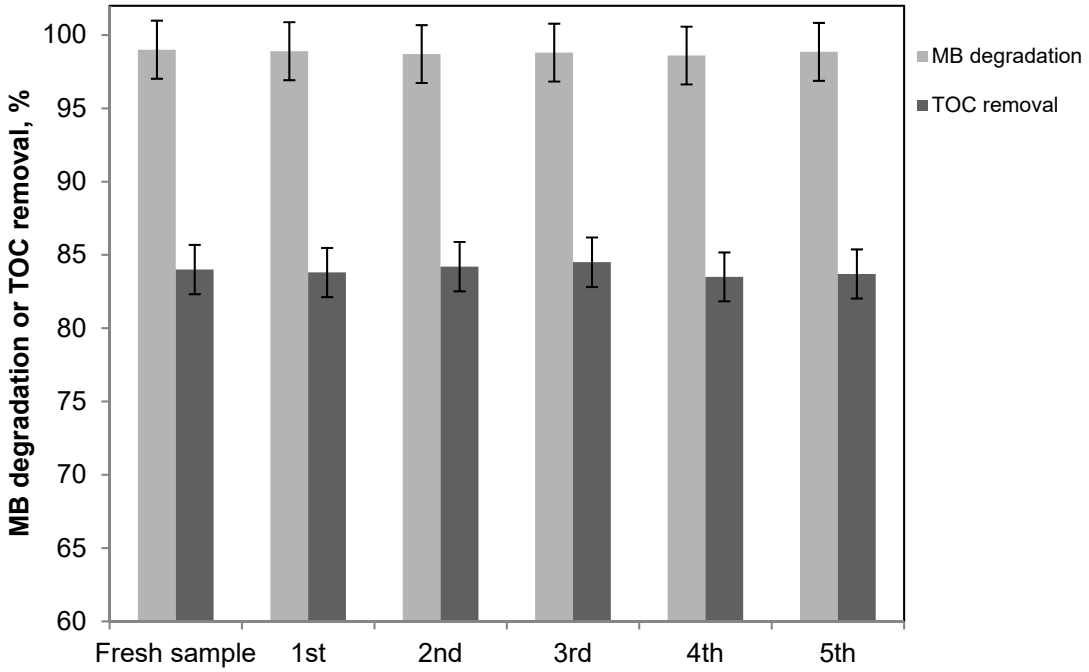

Figure 4. MB degradation and TOC removal after 300 min of irradiation at different repetitions. Light sources: visible LEDs; light intensity: 78 mW/cm^2; initial MB concentration: 7 mg/L; liquid flow rate: 50 mL/min; and photoreactor configuration: batch mode.

2.2. Photocatalytic Results on Methylene Blue Degradation with the Packed Bed photoreactor: Kinetic Evaluation and Mathematical Modelling

The mathematical modeling of the photocatalytic system, based on the use of the developed packed bed photoreactor at semi-pilot scale, has been performed using first order kinetics for MB photodegradation [41] and neglecting the external mass transfer phenomena. In order to verify this last hypothesis, the apparent kinetic constant was estimated from the experimental data collected using different liquid flow rates when the photoreactor operated in continuous mode (Figure 5) and at steady-state condition (Table 2).

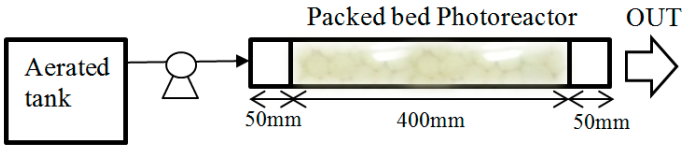

Figure 5. Schematic picture of the packed bed photoreactor working in in continuous mode.

Table 2. MB conversion at steady-state condition using different liquid flow rate when the photoreactor operated in continuous mode. Light sources: visible LEDs; light intensity: 78 mW/cm^2; and initial MB concentration: 7 mg/L.

Liquid Flow Rate (Q_0), mL/min	MB Conversion (X)
74.15	0.068
50	0.136
25.2	0.258
12.6	0.512
6.3	0.80

Considering the plug–flow behavior inside the packed bed, the MB mass balance can be written as:

$$Q_0 \times \frac{dX}{dW_{cat}} = K \times (1 - X) \quad (1)$$

where:

Q_0 = liquid flow rate, L/min;
K = apparent kinetic constant, L/(g min);
X = MB conversion;
W_{cat} = structured catalyst amount, g.

The boundary condition for Equation (1) is:

$W_{cat} = 0 : X = 0.$

Equation (1) is easily integrated obtaining the following relationship:

$$-\ln(1 - X) = K \times \frac{W_{cat}}{Q_0} \quad (2)$$

Figure 6 reports the behavior of (–ln(1 − X)) as a function of W_{cat}/Q_0. The slope of the obtained straight line is the value of the apparent kinetic constant K (3×10^{-5} L/(g min)), which can be seen as the product between the kinetic constant and the light intensity at the external surface of the photoreactor (Equation (3)) [38]:

$$K = k_{kinetic} \times I, \quad (3)$$

where:

$k_{kinetic}$ = kinetic constant, L cm^2/(g min mW);
I = light intensity, mW/cm^2.

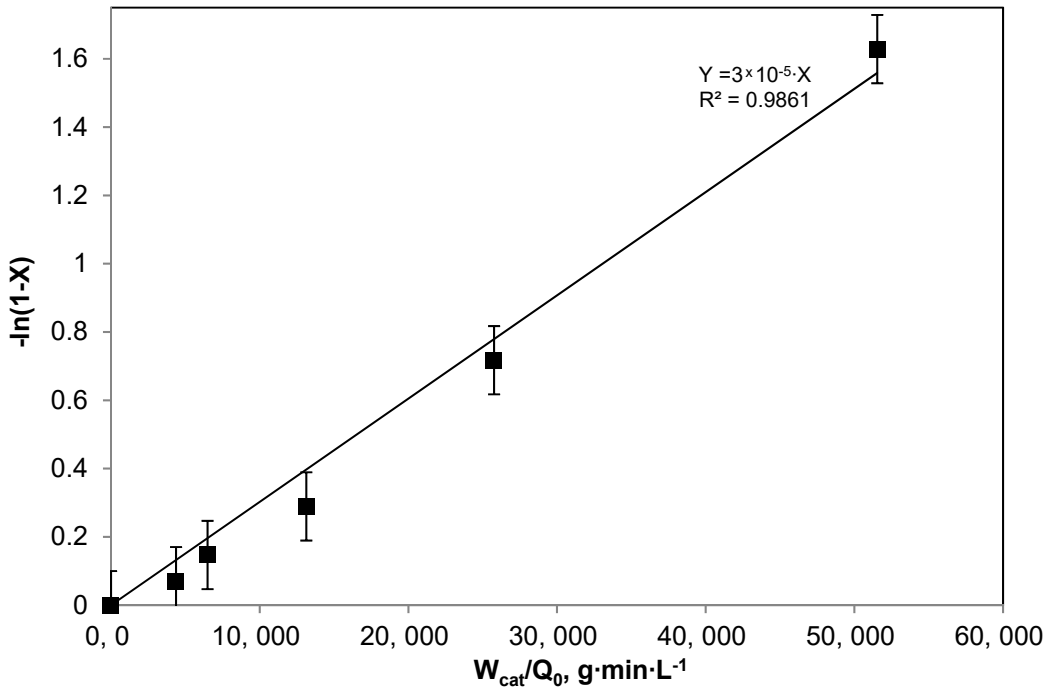

Figure 6. Evaluation of kinetic constant using photoreactor in continuous mode PFR (Plug Flow Reactor) at different liquid flow rate (in the range 6.3–74.15 mL/min). Light sources: visible LEDs; light intensity: 78 mW/cm^2; and initial MB concentration: 7 mg/L.

Considering the light intensity of 78 mW/cm^2, it was possible to evaluate the value of $k_{kinetic}$ from Equation (3), obtaining a value equal to 3.85×10^{-7} L cm^2/(g min mW).

The behaviour shown in Figure 6 confirmed the hypothesis that external mass transfer phenomena can be neglected since only one value of K is able to described the results obtained using different liquid flow rates [38,42].

The accuracy of the obtained value for $k_{kinetic}$ was verified by performing another series of experiments in which the visible light intensity was varied from 17.2 up to 78 mW/cm^2 to verify the ability of the model to predict experimental behaviour. In this case, the photoreactor operated in in batch mode, according to the schematic picture reported in Figure 1. In fact, the packed bed photoreactor was coupled with a tank, and the aqueous solution is continuously recirculated by means of the peristaltic pump for feeding the polluted water into the photoreactor. In this way, the reactor can be modeled like a batch system, as also reported in the literature concerning different photoreactor configurations for water and wastewater treatment [43].

Therefore, the MB mass balance can be written as:

$$\frac{dC}{dt} = -k_{kinetic} \cdot I \cdot \frac{W_{cat}}{V} \cdot C. \quad (4)$$

The initial condition for Equation (4) is:

$t = 0$; $C = C_0$,

where:

C_0 = MB initial concentration, mg/L;
C = MB concentration at the generic irradiation time, mg/L;
V = treated solution volume, L;
W_{cat} = structured catalyst amount, g.

Considering the mass balance on MB (Equation (4)) and integrating it between initial time ($t = 0$) and generic irradiation time t, it was obtained:

$$\frac{C}{C_o} = e^{-\left(\frac{k_{kinetic} \cdot I \cdot W_{cat}}{V}\right) \cdot t} \quad (5)$$

The value of $k_{kinetic}$, calculated from Equation (3) was used in Equation (5), and the calculated values of MB relative concentration as a function of irradiation time were compared with the experimental results collected at different light intensities (Figure 7).

As expected, the photocatalytic performances increased with the visible light intensity and the results obtained by the mathematical model were in agreement with the experimental results, evidencing the ability of the mathematical model to be predictive.

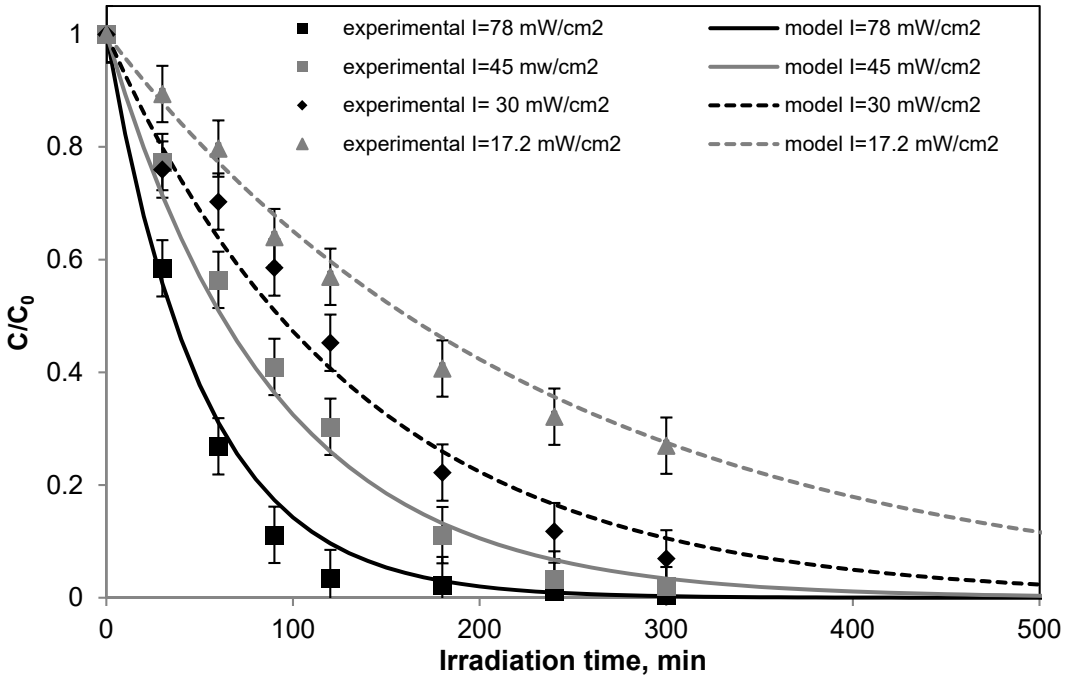

Figure 7. Comparison between experimental data and model calculation at different light intensity. Light sources: visible LEDs; initial MB concentration: 7 mg/L; liquid flow rate: 50 mL/min; and photoreactor configuration: batch mode.

2.3. Degradation and Mineralization of Ceftriaxone, Paracetamol, and Caffeine with the Packed Bed Photoreactor

The efficiency of the packed bed photoreactor was also evaluated in the removal of water pollutants of emerging concern, like pharmaceuticals and personal care products (PPCPs) [44–46]. The molecules tested in the present study were selected among the emerging pollutants detected in some Italian rivers and lakes and to represent different classes of PPCPs [47]. More precisely, ceftriaxone (CFX), caffeine (CAF), and paracetamol (PC) were chosen for photocatalytic tests. CFX is a long-acting, broad-spectrum cephalosporin antibiotic for parenteral use [48]. CF is a well-known compound used in pharmaceutical formulations as a stimulant and, moreover, is the most widely consumed psychoactive drug [49]. Finally, PC, also known as acetaminophen, is the compound used in many analgesic and antipyretic medicines [49]. For the photocatalytic tests on CFX, CAF, and PC, the packed bed photoreactor was used operating in batch mode. The initial concentration value for all PPCPs was mg/L. The obtained results are depicted in Figure 8. It was possible to observe a progressive decrease of the pollutants concentration during the irradiation time, evidencing that the photocatalytic system was effective in the removal of all the tested PPCPs.

In particular, for CFX, CAF, and PC, similar degradation degree (about 99% for CFX, 95% for CAF, and 99% for PC) and TOC removal (about 85% for CFX, 80% for CAF, and 83% for PC) were achieved after 180 min of visible light irradiation (Figure 9). Considering the literature concerning the degradation of CFX, PC, and CAF, it must be underlined that the most studied photocatalysts are used in powder form [49,50], making their use on an industrial scale very difficult. However, some studies have also reported the immobilization of photocatalyst particles on different macroscopic supports [50,51]. In particular, in the case of CFX, it has been shown that the studied structured photocatalyst is able to degrade the target molecule under UV irradiation for treatment time similar to those observed in our system, but the mineralization degree similar to our paper was achieved for 420 min irradiation time [52]. In addition, Miranda–Garcia et al., studying the degradation of the CAF and PC in a pilot compound parabolic collector (CPC) solar plant, observed that the photoactivity progressively worsened in five reuse cycles [51]. On the contrary, in our work, the same batch of

N-TiO_2/PS catalyst was instead used for the different PPCPs removal tests, indicating a good stability of the structured photocatalyst.

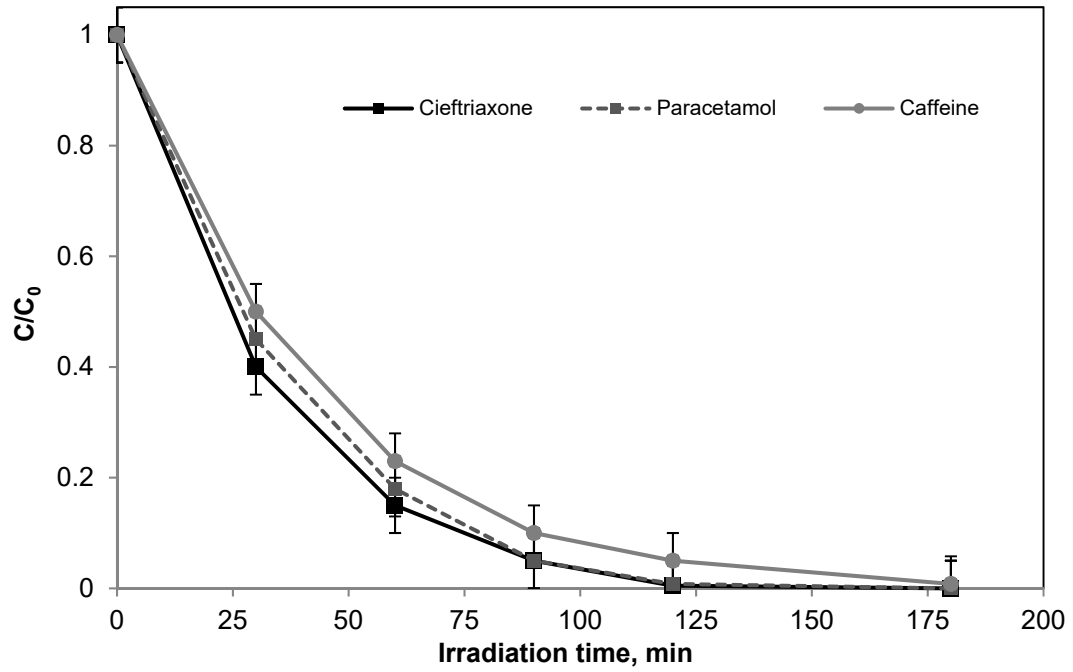

Figure 8. Behavior of ceftriaxone (CFX), paracetamol (PC), and caffeine (CAF) relative concentration as a function of irradiation time. Light sources: visible LEDs; light intensity: 78 mW/cm^2; initial pollutant concentration: 5 mg/L; liquid flow rate: 50 mL/min; and photoreactor configuration: batch mode.

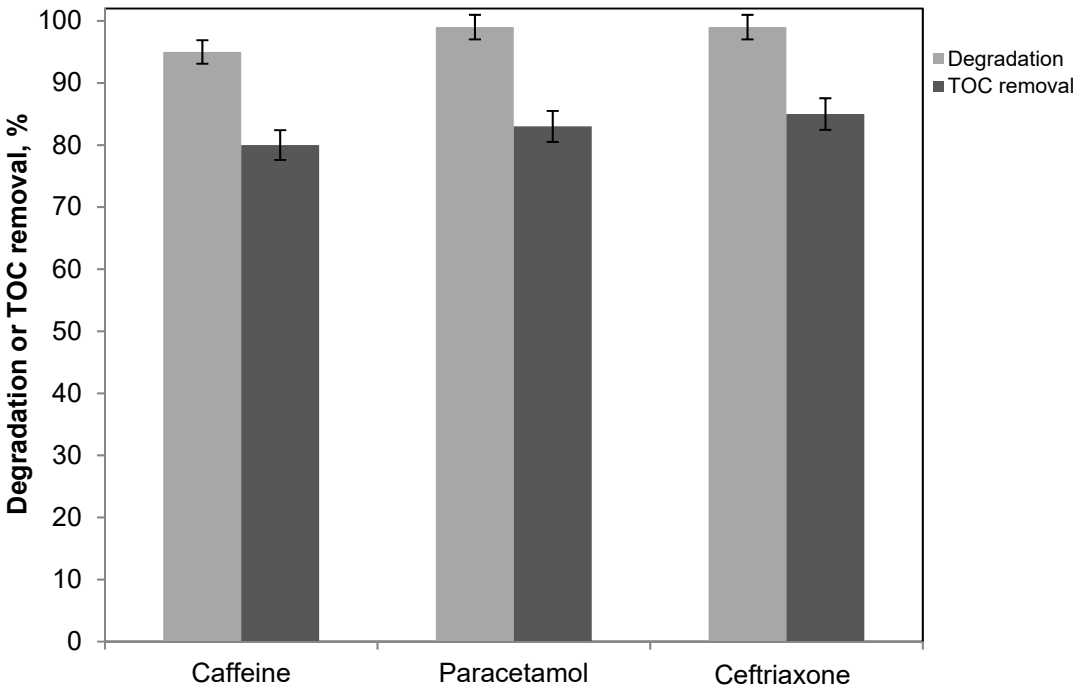

Figure 9. Pollutants degradation and TOC removal after 180 min of irradiation. Light sources: visible LEDs; light intensity: 78 mW/cm^2; initial pollutant concentration: 5 mg/L; liquid flow rate: 50 mL/min; and photoreactor configuration: batch mode.

3. Materials and Methods

3.1. Preparation of the Structured Photocatalyst

The Nitrogen-doped TiO_2 (N-TiO_2) photocatalyst was obtained by direct nitration during the hydrolysis of titanium tetraisopropoxide with ammonia aqueous solutions and calcination in air at 450 °C for 30 min. The N/Ti molar ratio in the prepared sample was 18.6 and corresponded to an optimized catalyst formulation found in our previous work [41]. The N-TiO_2 catalyst has been already characterized evidencing that the main crystallographic phase is antase and the band-gap energy is equal to 2.5 eV [41,53].

The polymeric supports used for the deposition of N-TiO_2 particles were PS spheres (mean diameter: 12 mm) [33]. The PS spheres were used as substrate for the deposition of N-TiO_2 powder using the solvent-casting method [54], according to the method reported in our previous work [32,33]. In particular, a certain quantity of N-TiO_2 photocatalyst was added to pure acetone and the suspension vigorously mixed until a uniform dispersion was obtained. Subsequently, the PS spheres were added to the obtained suspension in order to immobilize N-TiO_2 particles on the PS surface (N-TiO_2/PS). The spheres were then removed from the solution and dried at room temperature. In order to remove the N-TiO_2 particles that were not adhering to the PS spheres, several cycles in an ultrasonic bath (CEIA-CP104) were performed until a stable loading of the sample was reached. The amount of N-TiO_2 on the PS spheres was measured using precision balance (Mettler Toledo), and the final loading of N-TiO_2 in N-TiO_2/PS sample was found to be 1.7 wt% [33]. The structured N-TiO_2/PS photocatalyst was characterized by spectroscopic and morphological techniques in our previous work, evidencing that the preparation method was able to uniformly disperse N-doped TiO_2 particles in anatase phase on PS spheres and that the structured catalyst was active under visible and solar light [32,33]. No alteration of the N-TiO_2 photocatalytic activity was found after the supporting procedure.

3.2. Photocatalytic Tests with the Packed Bed Photoreactor at Semi-Pilot Scale

The experimental setup (Figures 1 and 5) consists of a packed bed photocatalytic reactor, an external stirred aerated tank containing the polluted solution, and a peristaltic pump to provide a continuous flow of water along the photocatalytic reactor.

The packed bed reactor included a cylindrical Pyrex tube to maximize the incident radiation intensity (40 cm long, 5 cm external diameter) and N-TiO_2/PS structured photocatalyst (325 g) as packing material. The photocatalytic experiments were conducted in both continuous mode (Figure 5) and batch mode (Figure 1). For both working conditions, the liquid flow rate was varied in the range 6.3–74.15 mL/min. In the case of batch mode, the total volume of the treated solution was 500 mL. The external body of the photoreactor was irradiated by an LEDs strip (produced by LED lighthouse; electrical power: 81.6 W) closely enwrapped around the external surface of the photoreactor (Figure 10). The emission spectrum of the LEDs lies in the range from 400 to 700 nm (Figure 10 insert).

The photocatalytic tests were carried out using MB at 10 mg/L initial concentration. Additional photocatalytic tests were carried out using aqueous solutions containing CAF, PC, and CFX at 5 mg/L initial concentration. The reactor was left in dark condition for 2 h before switching on visible LEDs.

All the photocatalytic tests were performed at the spontaneous pH of the polluted solutions, and the temperature was in the range 20–30 °C.

Liquid samples were analyzed by spectrophotometric measurements (Perkin Elmer UV-Vis spectrophotometer) in order to determine the concentration of MB (at λ = 663 nm), CAF (at λ = 273 nm) [55], PC (at λ = 246 nm) [50], and CFX (at λ = 254 nm) [56].

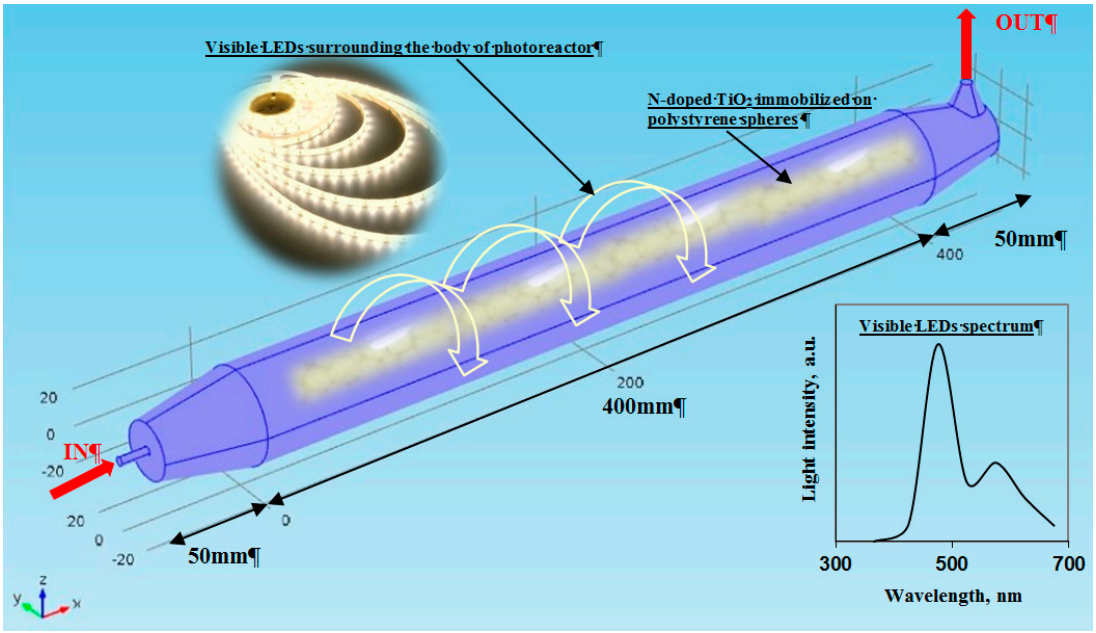

Figure 10. Schematic picture of the packed bed photoreactor configuration and the emission spectrum of the visible light LEDs strip (insert).

The TOC contained in a fixed volume of the solution was measured by the high temperature combustion method on a catalyst (Pt-Al_2O_3) in a tubular flow micro-reactor operated at 680 °C. The solution was injected in the catalytic reactor fed with air to oxidize the organic carbon into CO_2, whose concentration in gas–phase was monitored by a continuous analyzer (Uras 14, ABB) [6].

4. Conclusions

In this work, a packed bed photoreactor at semi-pilot scale was developed, using a visible light active structured photocatalyst. The packed bed reactor was irradiated by visible LEDs for the evaluation of photocatalytic activity in the removal of MB dye, as well as CFX, PC, and CAF, which are considered pollutants of emerging concern.

Photocatalytic tests driven in batch configuration showed that the N-TiO_2/PS photocatalyst was active in the photocatalytic degradation of MB, reaching almost total MB degradation after 120 min of irradiation, while no significant decrease in MB concentration was observed during the overall irradiation time in the absence of the structured catalyst. No influence of liquid flow rate was observed confirming that the overall MB photocatalytic degradation rate is mainly controlled by kinetics. A mathematical model for the photocatalytic degradation of MB was developed neglecting the external mass transfer phenomena. In order to verify this last hypothesis, the apparent kinetic constant was estimated from the experimental data collected, using different liquid flow rates when the photoreactor operated in continuous mode and at steady-state condition. The accuracy of the obtained value for the kinetic constant was verified by performing another series of experiments in which the visible light intensity varied. Finally, the efficiency of packed bed photoreactor at semi-pilot scale was also evaluated in the removal of CFX, CAF, and PC. The obtained results showed that the almost total degradation of the pollutants with a TOC removal more than 80% was achieved after 180 min of visible light irradiation. As concluding remarks, the obtained results are an encouraging step forward in the possible application of photocatalytic technology based on the use of visible LEDs and visible light structured photocatalysts in the elimination of hazard environmental pollutants, especially for the degradation of emerging bio-recalcitrant organic pollutants.

Author Contributions: O.S. performed the experiments and wrote the manuscript. V.V. provided the concept and experimental design of the study and reviewed the paper prior to submission. All authors discussed the results, analyzed the data and commented on the manuscript.

Funding: This research received no external funding.

Conflicts of Interest: The authors declare no conflict of interest.

References

1. Ho, Y.C.; Show, K.Y.; Guo, X.X.; Norli, I.; Abbas, F.M.A.; Morad, N. *Industrial Discharge and Their Effect to the Environment*; InTech: London, UK, 2012; pp. 1–32.
2. Koch, M.; Yediler, A.; Lienert, D.; Insel, G.; Kettrup, A. Ozonation of hydrolyzed azo dye reactive yellow 84 (ci). *Chemosphere* **2002**, *46*, 109–113. [CrossRef]
3. Can, O.T.; Kobya, M.; Demirbas, E.; Bayramoglu, M. Treatment of the textile wastewater by combined electrocoagulation. *Chemosphere* **2006**, *62*, 181–187. [CrossRef] [PubMed]
4. Gogate, P.R.; Pandit, A.B. A review of imperative technologies for wastewater treatment. Ii: Hybrid methods. *Adv. Environ. Res.* **2004**, *8*, 553–597. [CrossRef]
5. Panizza, M.; Brillas, E.; Comninellis, C. Application of boron-doped diamond electrodes for wastewater treatment. *J. Environ. Eng. Manag.* **2008**, *18*, 139–153.
6. Sannino, D.; Vaiano, V.; Ciambelli, P.; Isupova, L.A. Mathematical modelling of the heterogeneous photo-fenton oxidation of acetic acid on structured catalysts. *Chem. Eng. J.* **2013**, *224*, 53–58. [CrossRef]
7. Yu, L.; Chen, J.; Liang, Z.; Xu, W.; Chen, L.; Ye, D. Degradation of phenol using Fe_3O_4-GO nanocomposite as a heterogeneous photo-fenton catalyst. *Sep. Purif. Technol.* **2016**, *171*, 80–87. [CrossRef]
8. Saleh, R.; Taufik, A. Degradation of methylene blue and congo-red dyes using fenton, photo-fenton, sono-fenton, and sonophoto-fenton methods in the presence of iron(ii,iii) oxide/zinc oxide/graphene (Fe_3O_4/ZnO/graphene) composites. *Sep. Purif. Technol.* **2019**, *210*, 563–573. [CrossRef]
9. Rajasulochana, P.; Preethy, V. Comparison on efficiency of various techniques in treatment of waste and sewage water—A comprehensive review. *Resour. Effic. Technol.* **2016**, *2*, 175–184. [CrossRef]
10. Liu, Z.; Liang, Z.; Wu, S.; Liu, F. Treatment of municipal wastewater by a magnetic activated sludge device. *Desalin. Water Treat.* **2015**, *53*, 909–918. [CrossRef]
11. Maicu, M.; Hidalgo, M.C.; Colón, G.; Navío, J.A. Comparative study of the photodeposition of pt, au and pd on pre-sulphated TiO_2 for the photocatalytic decomposition of phenol. *J. Photochem. Photobiol. A Chem.* **2011**, *217*, 275–283. [CrossRef]
12. Herrmann, J.-M. Heterogeneous photocatalysis: Fundamentals and applications to the removal of various types of aqueous pollutants. *Catal. Today* **1999**, *53*, 115–129. [CrossRef]
13. Sacco, O.; Vaiano, V.; Matarangolo, M. Zno supported on zeolite pellets as efficient catalytic system for the removal of caffeine by adsorption and photocatalysis. *Sep. Purif. Technol.* **2018**, *193*, 303–310. [CrossRef]
14. Kim, S.-H.; Ngo, H.H.; Shon, H.K.; Vigneswaran, S. Adsorption and photocatalysis kinetics of herbicide onto titanium oxide and powdered activated carbon. *Sep. Purif. Technol.* **2008**, *58*, 335–342. [CrossRef]
15. Chakraborty, S.; Loutatidou, S.; Palmisano, G.; Kujawa, J.; Mavukkandy, M.O.; Al-Gharabli, S.; Curcio, E.; Arafat, H.A. Photocatalytic hollow fiber membranes for the degradation of pharmaceutical compounds in wastewater. *J. Environ. Chem. Eng.* **2017**, *5*, 5014–5024. [CrossRef]
16. Ray, A.K. A new photocatalytic reactor for destruction of toxic water pollutants by advanced oxidation process. *Catal. Today* **1998**, *44*, 357–368. [CrossRef]
17. Plakas, K.V.; Sarasidis, V.C.; Patsios, S.I.; Lambropoulou, D.A.; Karabelas, A.J. Novel pilot scale continuous photocatalytic membrane reactor for removal of organic micropollutants from water. *Chem. Eng. J.* **2016**, *304*, 335–343. [CrossRef]
18. Jafarikojour, M.; Dabir, B.; Sohrabi, M.; Royaee, S.J. Application of a new immobilized impinging jet stream reactor for photocatalytic degradation of phenol: Reactor evaluation and kinetic modelling. *J. Photochem. Photobiol. A Chem.* **2018**, *364*, 613–624. [CrossRef]
19. Lazar, M.A.; Varghese, S.; Nair, S.S. Photocatalytic water treatment by titanium dioxide: Recent updates. *Catalysts* **2012**, *2*, 572–601. [CrossRef]
20. Bhatkhande, D.S.; Kamble, S.P.; Sawant, S.B.; Pangarkar, V.G. Photocatalytic and photochemical degradation of nitrobenzene using artificial ultraviolet light. *Chem. Eng. J.* **2004**, *102*, 283–290. [CrossRef]

21. Borges, M.E.; Sierra, M.; Esparza, P. Solar photocatalysis at semi-pilot scale: Wastewater decontamination in a packed-bed photocatalytic reactor system with a visible-solar-light-driven photocatalyst. *Clean Technol. Environ. Policy* **2017**, *19*, 1239–1245. [CrossRef]
22. Rönnelid, M.; Perers, B.; Karlsson, B. Construction and testing of a large-area cpc-collector and comparison with a flat plate collector. *Sol. Energy* **1996**, *57*, 177–184. [CrossRef]
23. Malato, S.; Blanco, J.; Vidal, A.; Richter, C. Photocatalysis with solar energy at a pilot-plant scale: An overview. *Appl. Catal. B Environ.* **2002**, *37*, 1–15. [CrossRef]
24. Blanco, J.; Fernandez-Ibanez, P.; Malato-Rodríguez, S. Solar Photocatalytic Detoxification and Disinfection of Water: Recent Overview. *J. Sol. Energy Eng.* **2006**, *129*, 4–15. [CrossRef]
25. Abdel-Maksoud, Y.; Imam, E.; Ramadan, A. TiO_2 solar photocatalytic reactor systems: Selection of reactor design for scale-up and commercialization—Analytical review. *Catalysts* **2016**, *6*, 138. [CrossRef]
26. Jo, W.-K.; Tayade, R.J. New generation energy-efficient light source for photocatalysis: Leds for environmental applications. *Ind. Eng. Chem. Res.* **2014**, *53*, 2073–2084. [CrossRef]
27. Gan, W.Y.; Friedmann, D.; Amal, R.; Zhang, S.; Chiang, K.; Zhao, H. A comparative study between photocatalytic and photoelectrocatalytic properties of pt deposited TiO_2 thin films for glucose degradation. *Chem. Eng. J.* **2010**, *158*, 482–488. [CrossRef]
28. Casado, C.; Timmers, R.; Sergejevs, A.; Clarke, C.T.; Allsopp, D.W.E.; Bowen, C.R.; van Grieken, R.; Marugán, J. Design and validation of a led-based high intensity photocatalytic reactor for quantifying activity measurements. *Chem. Eng. J.* **2017**, *327*, 1043–1055. [CrossRef]
29. Pierpaoli, M.; Favoni, O.; Fava, G.; Ruello, M.L. A novel method for the combined photocatalytic activity determination and bandgap estimation. *Methods Protoc.* **2018**, *1*, 22. [CrossRef]
30. Hajaghazadeh, M.; Vaiano, V.; Sannino, D.; Kakooei, H.; Sotudeh-Gharebagh, R. Influence of operating parameters on gas phase photocatalytic oxidation of methyl-ethyl-ketone in a light emitting diode (led)-fluidized bed reactor. *Korean J. Chem. Eng.* **2015**, *32*, 636–642. [CrossRef]
31. Romero, R.L.; Alfano, O.M.; Cassano, A.E. Cylindrical photocatalytic reactors. Radiation absorption and scattering effects produced by suspended fine particles in an annular space. *Ind. Eng. Chem. Res.* **1997**, *36*, 3094–3109. [CrossRef]
32. Ata, R.; Sacco, O.; Vaiano, V.; Rizzo, L.; Tore, G.Y.; Sannino, D. Visible light active N-doped TiO_2 immobilized on polystyrene as efficient system for wastewater treatment. *J. Photochem. Photobiol. A Chem.* **2017**, *348*, 255–262. [CrossRef]
33. Sacco, O.; Vaiano, V.; Rizzo, L.; Sannino, D. Photocatalytic activity of a visible light active structured photocatalyst developed for municipal wastewater treatment. *J. Clean. Prod.* **2018**, *175*, 38–49. [CrossRef]
34. Sutisna; Rokhmat, M.; Wibowo, E.; Murniati, R.; Khairurrijal; Abdullaha, M. Novel solar photocatalytic reactor for wastewater treatment. *IOP Conf. Ser. Mater. Sci. Eng.* **2017**, *214*, 012010. [CrossRef]
35. El-Mekkawi, D.M.; Nady, N.; Abdelwahab, N.A.; Mohamed, W.A.A.; Abdel-Mottaleb, M.S.A. Flexible bench-scale recirculating flow cpc photoreactor for solar photocatalytic degradation of methylene blue using removable TiO_2 immobilized on pet sheets. *Int. J. Photoenergy* **2016**, *2016*, 9270499. [CrossRef]
36. Cunha, D.L.; Marques, M.; Kuznetsov, A.; Achete, C.A.; Machado, A.E.D.H. Immobilized TiO_2 on glass spheres applied to heterogeneous photocatalysis: Photoactivity, leaching and regeneration process. *PeerJ* **2018**, *6*, e4464. [CrossRef] [PubMed]
37. Sutisna; Rokhmat, M.; Wibowo, E.; Khairurrijal; Abdullah, M. Prototype of a flat-panel photoreactor using tio2 nanoparticles coated on transparent granules for the degradation of methylene blue under solar illumination. *Sustain. Environ. Res.* **2017**, *27*, 172–180. [CrossRef]
38. Vaiano, V.; Sacco, O.; Pisano, D.; Sannino, D.; Ciambelli, P. From the design to the development of a continuous fixed bed photoreactor for photocatalytic degradation of organic pollutants in wastewater. *Chem. Eng. Sci.* **2015**, *137*, 152–160. [CrossRef]
39. Sampaio, M.J.; Silva, C.G.; Silva, A.M.T.; Faria, J.L. Kinetic modelling for the photocatalytic degradation of phenol by using TiO_2-coated glass raschig rings under simulated solar light. *J. Chem. Technol. Biotechnol.* **2016**, *91*, 346–352. [CrossRef]
40. Vaiano, V.; Sarno, G.; Sacco, O.; Sannino, D. Degradation of terephthalic acid in a photocatalytic system able to work also at high pressure. *Chem. Eng. J.* **2017**, *312*, 10–19. [CrossRef]

41. Sacco, O.; Stoller, M.; Vaiano, V.; Ciambelli, P.; Chianese, A.; Sannino, D. Photocatalytic degradation of organic dyes under visible light on N-doped TiO_2 photocatalysts. *Int. J. Photoenergy* **2012**, *2012*, 626759. [CrossRef]
42. Perego, C.; Peratello, S. Experimental methods in catalytic kinetics. *Catal. Today* **1999**, *52*, 133–145. [CrossRef]
43. De Lasa, H.; Serrano, B.; Salaices, M. *Photocatalytic Reaction Engineering*; Springer Science+Business Media: New York, NY, USA, 2005. [CrossRef]
44. Heberer, T. Occurrence, fate, and removal of pharmaceutical residues in the aquatic environment: A review of recent research data. *Toxicol. Lett.* **2002**, *131*, 5–17. [CrossRef]
45. Mahdizadeh, F.; Aber, S.; Karimi, A. Synthesis of nano zinc oxide on granular porous scoria: Application for photocatalytic removal of pharmaceutical and textile pollutants from synthetic and real wastewaters. *J. Taiwan Inst. Chem. Eng.* **2015**, *49*, 212–219. [CrossRef]
46. Shaykhi, Z.M.; Zinatizadeh, A.A.L. Statistical modeling of photocatalytic degradation of synthetic amoxicillin wastewater (saw) in an immobilized TiO_2 photocatalytic reactor using response surface methodology (rsm). *J. Taiwan Inst. Chem. Eng.* **2014**, *45*, 1717–1726. [CrossRef]
47. Zuccato, E.; Calamari, D.; Natangelo, M.; Fanelli, R. Presence of therapeutic drugs in the environment. *Lancet* **2000**, *355*, 1789–1790. [CrossRef]
48. Ethiraj, R.; Sampath, V.S.; Vahid, A.; Raj, J.; Thiruvengadam, E. Development and validation of stability indicating spectroscopic method for content analysis of ceftriaxone sodium in pharmaceuticals. *Int. Sch. Res. Not.* **2014**, *2014*, 278173. [CrossRef] [PubMed]
49. Rimoldi, L.; Meroni, D.; Falletta, E.; Pifferi, V.; Falciola, L.; Cappelletti, G.; Ardizzone, S. Emerging pollutant mixture mineralization by TiO_2 photocatalysts. The role of the water medium. *Photochem. Photobiol. Sci.* **2017**, *16*, 60–66. [CrossRef] [PubMed]
50. Jallouli, N.; Elghniji, K.; Trabelsi, H.; Ksibi, M. Photocatalytic degradation of paracetamol on TiO_2 nanoparticles and TiO_2/cellulosic fiber under UV and sunlight irradiation. *Arab. J. Chem.* **2017**, *10*, S3640–S3645. [CrossRef]
51. Miranda-García, N.; Suárez, S.; Sánchez, B.; Coronado, J.M.; Malato, S.; Maldonado, M.I. Photocatalytic degradation of emerging contaminants in municipal wastewater treatment plant effluents using immobilized TiO_2 in a solar pilot plant. *Appl. Catal. B Environ.* **2011**, *103*, 294–301. [CrossRef]
52. Shokri, M.; Isapour, G.; Shamsvand, S.; Kavousi, B. Photocatalytic Degradation of Ceftriaxone in Aqueous Solutions by Immobilized TiO_2 and ZnO Nanoparticles: Investigating Operational Parameters. *J. Mater. Environ. Sci.* **2016**, *7*, 2843–2851.
53. Rizzo, L.; Sannino, D.; Vaiano, V.; Sacco, O.; Scarpa, A.; Pietrogiacomi, D. Effect of solar simulated N-doped TiO_2 photocatalysis on the inactivation and antibiotic resistance of an *E. coli* strain in biologically treated urban wastewater. *Appl. Catal. B Environ.* **2014**, *144*, 369–378. [CrossRef]
54. Siemann, U. Solvent cast technology—A versatile tool for thin film production. In *Scattering Methods and the Properties of Polymer Materials*; Stribeck, N., Smarsly, B., Eds.; Springer: Berlin/Heidelberg, Germany, 2005; pp. 1–14.
55. Elhalil, A.; Elmoubarki, R.; Farnane, M.; Machrouhi, A.; Sadiq, M.; Mahjoubi, F.Z.; Qourzal, S.; Barka, N. Photocatalytic degradation of caffeine as a model pharmaceutical pollutant on mg doped ZnO-Al_2O_3 heterostructure. *Environ. Nanotechnol. Monit. Manag.* **2018**, *10*, 63–72. [CrossRef]
56. Zhao, Y.; Liang, X.; Wang, Y.; Shi, H.; Liu, E.; Fan, J.; Hu, X. Degradation and removal of ceftriaxone sodium in aquatic environment with Bi_2WO_6/g-C_3N_4 photocatalyst. *J. Colloid Interface Sci.* **2018**, *523*, 7–17. [CrossRef] [PubMed]